ANALYSIS OF THE FLOW AROUND AN OSCILLATING CIRCULAR CYLINDER IN GROUND EFFECT

Washington Humberto de Moura
Instituto de Engenharia Mecânica, UNIFEI, CP 50, Itajubá, Minas Gerais, 37500-903, Brasil
e-mail: whmoura@unifei.edu.br

Hélia Silva
Instituto de Engenharia Mecânica, UNIFEI, CP 50, Itajubá, Minas Gerais, 37500-903, Brasil
e-mail: heva@unifei.edu.br

Luiz Antonio Alcântara Pereira
Instituto de Engenharia Mecânica, UNIFEI, CP 50, Itajubá, Minas Gerais, 37500-903, Brasil
e-mail: luizantp@unifei.edu.br

Miguel Hiroo Hirata
FAT/UERJ
Campus Regional de Resende
Estrada Resende - Riachuelo, Resende, RJ
e-mail: hirata@fat.uerj.br

Abstract. *The aim of this work is to simulate numerically the two-dimensional, incompressible Newtonian fluid flow around a circular cylinder oscillating with small amplitude in the presence of ground plane. The vorticity generated on the body surface interacts with the vorticity generated on the ground plane surface to form the viscous wake; the vorticity is discretized and is numerically simulated using discrete Lamb vortices. The influence of the clearance and of the amplitude oscillation on the aerodynamics loads are analyzed.*

Keywords: vortex method, panels methods, ground effect, small amplitude, aerodynamics loads, lagrangian description.

1. Introduction

The analysis of the unsteady vorticity-dominated flow is a long-standing interest of many researches. In this paper we consider one small aspect of the total problem: the numerical simulation of the wake generated by an oscillating circular cylinder, which moves with constant velocity in the presence of a ground plane. The amplitude of the oscillatory motion is considered to be small compared to the body length; therefore, to the first approximation one is allowed to transfer the body boundary condition from the actual position to a mean position of the body surface. The numerical simulation is accomplished by using the Vortex Method, which takes into account the viscous effect in the flow field.

Oscillatory motions of small amplitude are important in the analysis of immerse vibrating bodies and special care should be taken in the lock-in condition.

The problem described can be compared with many engineering situations where is possible verify changes in the velocity field around a body thus a surface localized near the neighborhood. An automobile near the ground and an aircraft landing or taking off are examples of this phenomenon.

In the literature a model of the single airfoil, near a ground plane, immersed in an upstream shear flow is referred to as "the airfoil-vortex interaction in ground effect" – AVIG – and can be viewed as a combination of three interacting flows: airfoil-vortex interaction (AVI), airfoil-ground interaction (AGI), and vortex-ground interaction (VGI). A large number of papers on the unsteady, incompressible, two-dimensional AVI flow have been published. Within the context of the (two-dimensional) parallel AVI that occurs around helicopter rotors, known as blade-vortex interaction (BVI), Panaras (1987), Poling *et al.* (1989) and Lee and Smith (1991), among others, have devised numerical models based on the inviscid discrete vortex method coupled with linearized potential flow theory. More elaborate numerical models have also been employed, such as those based on Euler (Srinivasan and McCroskey, 1993) and Navier-Stokes (Rai, 1987) mesh-based methods. Detailed experimental investigations on the aerodynamics of parallel BVI have been performed by Seath *et al.* (1989), Straus *et al.* (1990), Chen and Chang (1997). See the review articles of McCune and Tavares (1993) and Mook and Dong (1994) for additional references on unsteady, incompressible flows over airfoils and the numerical simulation of wakes and BVI.

Chacaltana *et al.* (1995) analyze the flow around a thin airfoil immersed in a shear flow, in presence of a ground plane. The authors use the potential flow theory and taking into account the fact that the airfoil is thin were able to derive a simple algorithm. In this paper, the shear flow was simulated by a single moving free vortex.

Fonseca *et al.* (1997, 2003) in a series of two papers applied a numerical, inviscid, vortex method to simulate the unsteady, two-dimensional and incompressible flow that occurs during a parallel blade-vortex interaction in ground effect. A panel method was used to discretize the airfoil bound vorticity, where each panel has a linear and piecewise-continuous distribution of vorticity. The impermeability condition was enforced on the airfoil contour, but the no-slip condition is not. The Kutta condition was imposed through the continuity of the pressure field at the airfoil trailing edge, which, combined with the condition that the circulation in the whole flow must be conserved, provides a model for the vorticity generation at the trailing edge. Thus the viscous wake was modeled by potential vortices shed into the flow at the trailing edge and the oncoming shear flow was modeled by a single potential vortex that interacts with the airfoil and its wake.

Ricci *et al.* (2001) presented a new methodology that utilizes the Vortex Method for the analysis of the vorticity generated in the surface of the airfoil with that generated on the ground plane. Lamb vortices are generated along the airfoil surface and ground plane to ensure that the no-slip condition is satisfied. Images clouds are provided in the lower half ground to ensure that the impermeability condition is satisfied. With the images clouds the computation becomes expensive. This is a major source of difficulties, and it can only be handled through the utilization of method of distributed singularities, the Panels Method.

Silva de Oliveira *et al.* (2005) employed the Vortex Method to simulate the airfoil-vortex cloud interaction in ground effect. The no-slip condition is satisfied using Lamb vortices to simulate the vorticity generated in the airfoil surface and that generated in the ground surface. The impermeability condition is imposed through the application of a source panel method. The main feature of the paper is the oncoming shear flow that has two important characteristics. The first is that the shear flow is continuously generated is a plane perpendicular to the main flow, a feature not found in any of the previous paper, and the second characteristic is the possibility of having a time variation of the vorticity carried out by this shearing flow, see Silva de Oliveira *et al.* (2004).

Silva (2004) applied the Vortex Method to analyze the flow around an oscillating airfoil, which moves with constant velocity. The amplitude of the oscillatory motion is considered to be small compared to the airfoil length, therefore, to the first approximation, one is allowed to transfer the body boundary condition from the actual position to a mean position of the body surface. Aerodynamic loads are calculated using an integral equation derived from the pressure Poisson equation (Alcântara Pereira *et al.,* 2004). An analysis of the oscillation effect on the mechanism of lift generation is also presented. The influence of the ground effect is not considered.

As mentioned, the model is analyzed using the Vortex Method which is a meshless numerical method or a particle method. In this method, the vorticity in the fluid region is numerically simulated using a cloud of discrete vortices with a viscous core (Lamb vortex). To simulate the vorticity at the solid surfaces, nascent vortices are generated there at each time step of the simulation. In order to take care of the convection and the diffusion of the vorticity one makes use of the convection-diffusion splitting algorithm; accordingly the convection of the vortices in the cloud is carried out independently of the diffusion for each time step of the simulation. The convection process is carried out with the Adams-Bashforth time-marching scheme and the diffusion process is simulated using the random walk method. This is in essence the foundation of the Vortex Method (e.g. references Chorin, 1973; Sarpkaya, 1989; Sethian, 1991; Lewis, 1999; Alcântara Pereira *et al.*, 2002 and Kamemoto, 2004). Please note that with the Lagrangian formulation a grid for the spatial discretization of the fluid region is not necessary. Thus, special care to handle numerical instabilities associated to high Reynolds numbers is not needed. Also, the attention is only focused on the regions of high activities, which are the regions containing vorticity; on the contrary, Eulerian schemes consider the entire domain independent of the fact that there are sub-regions where less important, if any, flow activity can be found. With the Lagrangian tracking of the vortices, one need not take into account the far away boundary conditions. This is of important in the wake regions (which is not negligible in the flows of present interest) where turbulence activities are intense and unknown, a priori.

The present Vortex Method has been used to simulate the macro scale phenomena, therefore the smaller scale ones are taken into account through the use of a second order velocity function (Alcântara Pereira et *al*., 2002). In this present approach, the effect of small scale is not considered.

2. Description of the numerical model of the flowfield

2.1. Basic concepts

Consider the incompressible flow of a Newtonian fluid in a large two-dimensional domain around a circular cylinder which moves with constant velocity U in ground effect. An oscillatory moving with finite amplitude A and constant angular velocity ω is added to body as shown in Fig. 1. In this figure the (x, o, y) is the inertial frame of reference and the (X, O, Y) is the coordinate system fixed to the cylinder; this coordinate system oscillates around the x-axis as $y_o = A\cos(\omega t)$.

The boundary S of the fluid domain Ω is $S = S_1 \cup S_2 \cup S_3$; being S_3 the far away boundary, which can be viewed as $r = \sqrt{x^2 + y^2} \to \infty$, and S_1 the body surface and S_2 the ground plane surface.

In the body fixed coordinate system, the surface $S_1 \equiv S_b$ is defined by the function

$$F_b(X, Y) = Y_b - \eta(X) = 0 \tag{1}$$

Thus, in the inertial frame of reference

$$S_b : F_b(x, y, t) = y_b - [y_0(t) + \eta(x)] = 0 , \tag{2}$$

and, for a symmetrical body

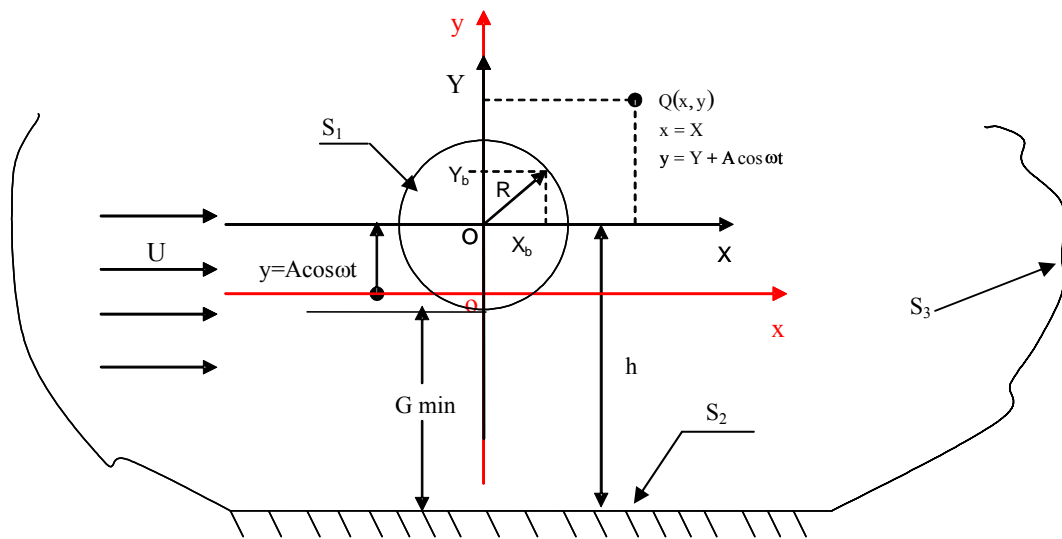$$F_b(x, y, t) = y_b - y_0(t) \mp \eta(x) = 0 . \tag{3}$$

Figure 1. Definitions.

The cylinder surface $S_1 \equiv S_b$ is defined according the following form

$$S_b(X, Y) = \sqrt{X^2 + Y^2} = R \tag{4}$$

and the boundary surface S_2 is defined as

$$y = -h, \ -\infty < x < \infty \tag{5}$$

2.2. Governing equations

The viscous and incompressible flow is governed by the continuity and the Navier-Stokes equations, which can be written in the form

$$\nabla \cdot \mathbf{u} = 0 \tag{6}$$

$$\frac{\partial \mathbf{u}}{\partial t} + \mathbf{u} \cdot \nabla \mathbf{u} = -\nabla p + \frac{1}{Re} \nabla^2 \mathbf{u} . \tag{7}$$

where $\mathbf{u} \equiv (u, v)$ is the velocity vector. As can be seen the equations are non-dimensionalized in terms of U and b (cylinder diameter: b = 2R). The Reynolds number is defined by

$$Re = \frac{bU}{\upsilon} \tag{7a}$$

where υ is the fluid kinematics viscosity coefficient; the dimensionless time is b/U.

On the body and ground plane surfaces the adherence condition has to be satisfied. This condition is better specified in terms of the normal and tangential components as

$$(\mathbf{u} \cdot \mathbf{n}) = (\mathbf{v} \cdot \mathbf{n}) \text{ on } S_1 \text{ and } S_2 \text{ , the impenetrability condition} \qquad (8a)$$

$$(\mathbf{u} \cdot \boldsymbol{\tau}) = (\mathbf{v} \cdot \boldsymbol{\tau}) \text{ on } S_1 \text{ and } S_2 \text{ , the impenetrability condition, the no-slip condition.} \qquad (8b)$$

Here $\mathbf{n}$ and $\boldsymbol{\tau}$ are unit normal and tangential vectors and v is the surfaces velocity: S_1 and S_2.

Far from the surfaces S_1 and S_2 one assumes that the perturbation due to the oscillating body fades away, that is

$$|\mathbf{u}| \to 1 \text{ at } S_3. \qquad (9)$$

Is considered an small amplitude around the axis x, therefore

$$\frac{A}{2R} = O(\varepsilon) \text{ , where } \varepsilon \to 0 \text{ and } \omega = O(1). \qquad (10)$$

Thus, the boundary conditions on S_1 are written directly in the inertial frame of reference as

$$u_n(x, y, t) \equiv \left[v_n(x, y, t) \right] \text{ on } S_1 \text{ , the impenetrability condition} \qquad (11a)$$

$$u_\tau(x, y, t) \equiv \left[v_\tau(x, y, t) \right] \text{ on } S_1 \text{ , the impenetrability condition .} \qquad (11b)$$

The transference of the boundary conditions on S_1 from actual position to the mean position is defined as

$$y_c = y_0 + \eta(x) \to \overline{y}_c = \eta(x) + O(y_0) \qquad (12a)$$

$$u_n(x_c, y_c, t) = u_n\left(x_c, y_0 + \eta, t\right) = u_n\left(x_c, \eta(x_c), t\right) + y_0 \frac{\partial u_n\left(x_c, \eta(x_c), t\right)}{\partial y} + \cdots \qquad (12b)$$

$$u_\tau(x_c, y_c, t) = u_\tau\left(x_c, y_0 + \eta, t\right) = u_\tau\left(x_c, \eta(x_c), t\right) + y_0 \frac{\partial u_\tau\left(x_c, \eta(x_c), t\right)}{\partial y} + \cdots \qquad (12c)$$

The dynamics of the fluid motion, governed by the above boundary-value problem, can be alternatively studied by taking the curl of Eq. (7), obtaining the well-known 2-D vorticity transport equation

$$\frac{\partial \omega}{\partial t} + \mathbf{u} \cdot \nabla \omega = \frac{1}{Re} \nabla^2 \omega \qquad (13)$$

where ω is the only non-zero component of the vorticity vector $\boldsymbol{\omega} = \nabla \times \mathbf{u}$.

2.3. Discrete vortex method

According to the convection-diffusion splitting algorithm (Chorin, 1973) it is assumed that in the same time increment the convection and the diffusion of the vorticity can be independently handled and are governed by

$$\frac{\partial \omega}{\partial t} + \mathbf{u} \cdot \nabla \omega = 0 \qquad (14)$$

$$\frac{\partial \omega}{\partial t} = \frac{1}{Re} \nabla^2 \omega .$$

(15)

Convection is governed by Eq. (14) and the velocity field is given by

$$u - iv = 1 + \frac{1}{2\pi} \sum_{n=1}^{2M} \sigma(S_n) \int_{\Delta S_n} \frac{d}{dz} \ln(z - \zeta) d\zeta + \frac{i}{2\pi} \sum_{k=1}^{N} \frac{\Delta \Gamma_k}{z - z_k} .$$

(16)

Here, u and v are the x and y components of the velocity vector $\mathbf{u}$ and $i = \sqrt{-1}$. The first term in the right hand sides is the contribution of the incident flow; the summation of $2M$ integral terms comes from the sources panels with constant density distributed on the circular cylinder and ground surfaces. The second summation is associated to the velocity induced by the cloud of N free vortices; it represents the vortex-vortex interactions.

The incident flow and the vortex-vortex interactions calculations present no problems and they follow the usual Vortex Method procedures; to the first approximation the same happens with the summation of $2M$ integral terms when the body (circular cylinder) oscillation amplitude is small, see Silva (2004). For large amplitude body oscillations, however, the body boundary conditions can not be transferred from the actual position to the mean position.

The fluid velocity on the circular cylinder surface is written as

$$\mathbf{u}(X, Y; t) = U\mathbf{i} - \dot{y}_0(t)\mathbf{j} \; ; \text{ with } \dot{y}_0(t) = \frac{d}{dt}\left[A\cos(\omega t)\right]$$

(17)

As a consequence of the j component of the right hand side of the fluid velocity (in the above expression) one gets an additional singularities distribution on the body surface. Of course, the induced velocity due to this additional singularities distribution fades away from the body.

The velocity induced by the body, according to the Panels Method calculations, is indicated by [uc(X,Y), vc(X,Y)]; this is the velocity induced at the vortex (i), located at the point [x(t), y(t)]; thus

$$uc^{(i)}(x, y; t) = uc(X, Y; t)$$

(18a)

$$vc^{(i)}(x, y; t) = vc(X, Y; t)$$

(18b)

where the following relations remains

$$x^{(i)}(t) = X$$

(19a)

$$y^{(i)}(t) = y_0(t) + Y$$

(19b)

The process of vorticity generation is carried out from Eq. (8b), so as to satisfy the no-slip condition. According to the discussion above the Panels Method guaranties that the impermeability condition is satisfied in each straight-line element, or panel, at pivotal point. At each instant of the time 2M new vortices are created a small distance ε of the body and ground plane surfaces, whose strengths are determined from Eq. (8b) applied at 2M point's right below the newly created vortices, along the radial direction. This procedure yields an algebraic system of 2M equations and 2M unknowns (the strengths of the vortices).

In order to remove the singularity in the second summation of Eq. (16) Lamb vortices are used, whose mathematical expression for the induced velocity of the kth vortex with strength $\Delta \Gamma_k$ in the circumferential direction u_{θ_k} , is (Mustto *et al.*, 1998)

$$u_{\theta_k} = \frac{\Delta \Gamma_k}{2\pi r} \left\{ 1 - \exp\left[-5.02572\left(-\frac{r}{\sigma_0} \right)^2 \right] \right\}$$

(20)

where σ_0 is core radius of the Lamb vortex.

In this particular equation r is the radial distance between the vortex center and the point in the flow field where the induced velocity is calculated.

Each vortex particle distributed in the flow field is followed during numerical simulation according to the Adams-Bashforth second-order formula (Ferziger, 1981)

$$z(t+\Delta t) = z(t) + [1.5u(t) - 0.5u(t-\Delta t)]\Delta t + \xi \qquad (21)$$

in which z is the position of a particle, Δt is the time increment and ξ is the random walk displacement. According to Lewis (1991), the random walk displacement is given by

$$\xi = \sqrt{4\beta\Delta t \ln\left(\frac{1}{P}\right)}[\cos(2\pi Q) + i\sin(2\pi Q)] \qquad (22)$$

where $\beta = Re^{-1}$; P and Q are random numbers between 0.0 and 1.0.

The pressure calculation starts with the Bernoulli function, defined by Uhlman (1992) as

$$Y = p + \frac{u^2}{2}, \quad u = |\mathbf{u}|. \qquad (23)$$

Kamemoto (1993) used the same function and starting from the Navier-Stokes equations was able to write a Poisson equation for the pressure. This equation was solved using a finite difference scheme. Here the same Poisson equation was derived and its solution was obtained through the following integral formulation (Shintani and Akamatsu, 1994)

$$H\overline{Y_i} - \int_{S_1} \overline{Y}\nabla G_i \cdot \mathbf{e}_n dS = \iint_\Omega \nabla G_i \cdot (\mathbf{u}\times\omega)d\Omega - \frac{1}{Re}\int_{S_1}(\nabla G_i \times \omega)\cdot\mathbf{e}_n dS \qquad (24)$$

where H is 1.0 inside the flow (at domain Ω) and is 0.5 on the boundaries S_1 and S_2. $G_i = (1/2\pi)\log R^{-1}$ is the fundamental solution of Laplace equation, R being the distance from ith vortex element to the field point.

It is worth to observe that this formulation is specially suited for a Lagrangian scheme because it utilizes the velocity and vorticity field defined at the position of the vortices in the cloud. Therefore it does not require any additional calculation at mesh points. Numerically, Eq. (24) is solved by mean of a set of simultaneous equations for pressure Y_i.

4. Results and conclusions

The numerical simulations were restricted to the flow around a circular cylinder and for the calculations each boundary S_1 and S_2 in Fig. (1) was represented by fifty (M=50) source panels; the time step and Reynolds number were taken as $\Delta t=0.05$ and $Re=10^5$, respectively. In each time step the nascent vortices were placed into the cloud through a displacement $\epsilon = \sigma_0 = 0.0009b$ normal to the panels. The aerodynamics forces computations starts at t=10.

Table 1: Strouhal number, lift and drag coefficients for a circular cylinder with h/b $\to\infty$.

$Re = 10^5$, A = 0 and $\omega = 0$	$\overline{C}_L$	$\overline{C}_D$	$\overline{S}_t$
Blevins (1984)	-	1.20	0.19
Mustto *et al.* (1998)	-	1.22	0.22
Alcântara Pereira *et al.*(2002)	0.04	1.21	0.22
Present simulation	0.06	1.20	0.19

As first case we consider A=0, ω=0 and h/b $\to \infty$. The result of the first case is presented in Table 1. In this table one can find also experimental, Blevins (1984) (with 10% uncertainty) and numerical results Mustto *et al.* (1998). The numerical results of Mustto *et al.* (1998) were also obtained using the Vortex Method with the Circle Theorem (Milne-Thompson, 1955), while the Panels Method, using straight-line vortex panels with constant density, was used in the results of Alcântara Pereira *et al.* (2002). The agreement between the two numerical methods is very good for the Strouhal number, and both results are close to the experimental values. One should observe, however, that three-dimensional effects are non-negligible for the Reynolds number used in the simulations. Therefore one can expect that a

two-dimensional computation of such a flow must produce higher values for the drag coefficient. On the other hand, the Strouhal number is insensitive to these three-dimensional effects.
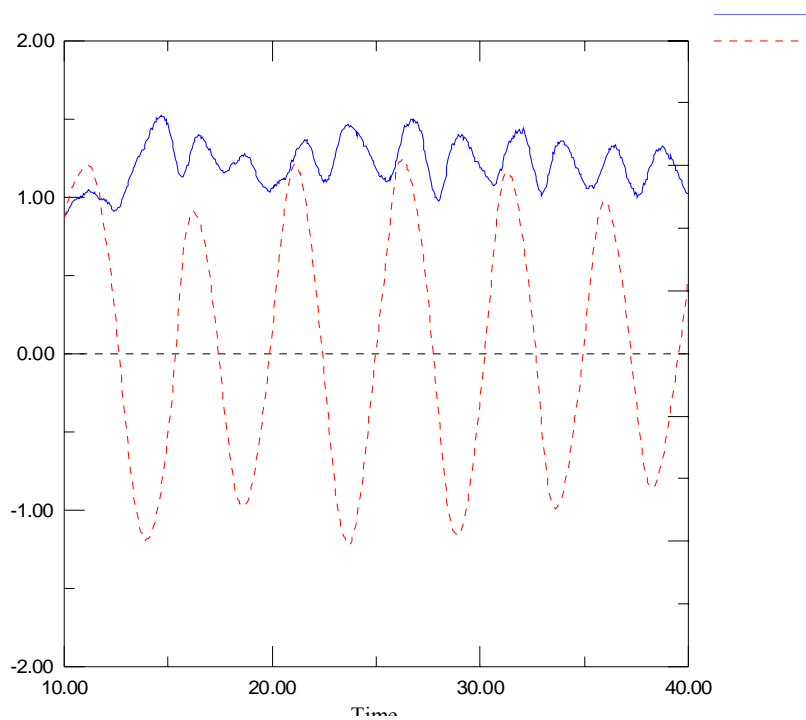

Figure 2: Circular cylinder: drag and lift coefficients during the numerical simulation; $A = 0$, $\omega = 0$ and $Re = 10^5$.

Figure 3 shows the mean value of pressure coefficient around the discretized circular cylinder surface. The present result is compared with others results available in the literature and current simulation agree very well with the experimental ones. From the simulation the predict separation points occur around 86°, while the experimental value is around 82°. In other experimental investigation by Son and Hanratty (1969); determined a value of 78° for the separation angle.
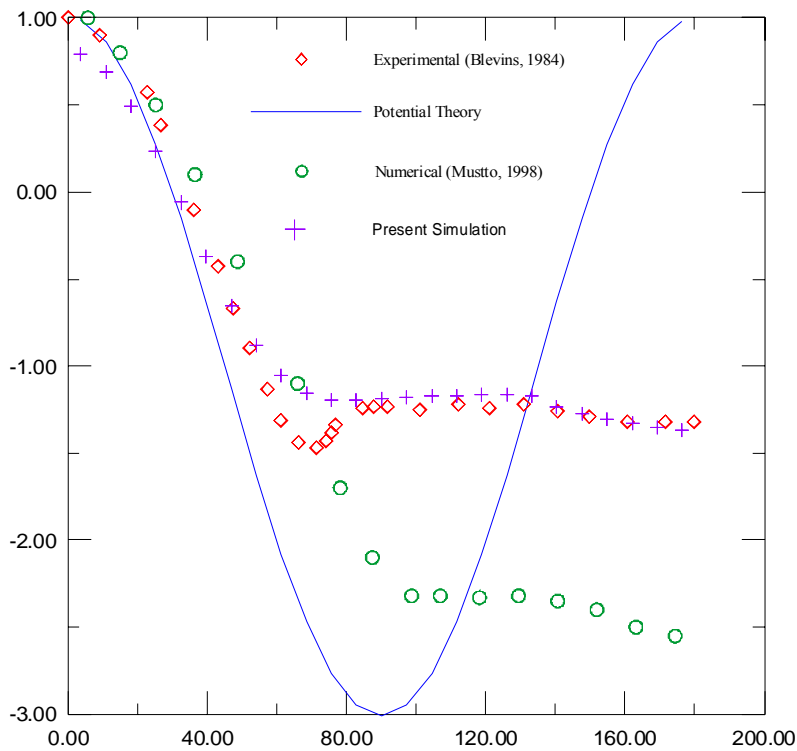

Figure 3. Comparison of the circular cylinder case, experimental and numerical results of C_p, for $A = 0$, $\omega = 0$, $Re=10^5$.

We believe that better approximation for the experimental curve and numerical curve is obtained increasing the number of panels to approximate the real surfaces. Also, use of the turbulence modeling (Alcântara Pereira *et al.,* 2002) will produce a better numerical result.

Figure 2 shows that the lift coefficient oscillates around zero, as expected. However the mean value is slightly different from zero.

The influence of the ground effect, with A = 0 and ω = 0, is preliminary investigated and presented in the Fig. 4. News simulations will be carried out to investigate the present phenomena. The numerical results seem to indicate that the higher value of N would improve the resolution and probably produce a better simulation with respect to the ground effect.

Table 2 shows samples of others results obtained. Case I presents the results for a stand still cylinder, while Cases II to XII represent typical values for small amplitude motions with ω = 1.0 and Re = 10^5.
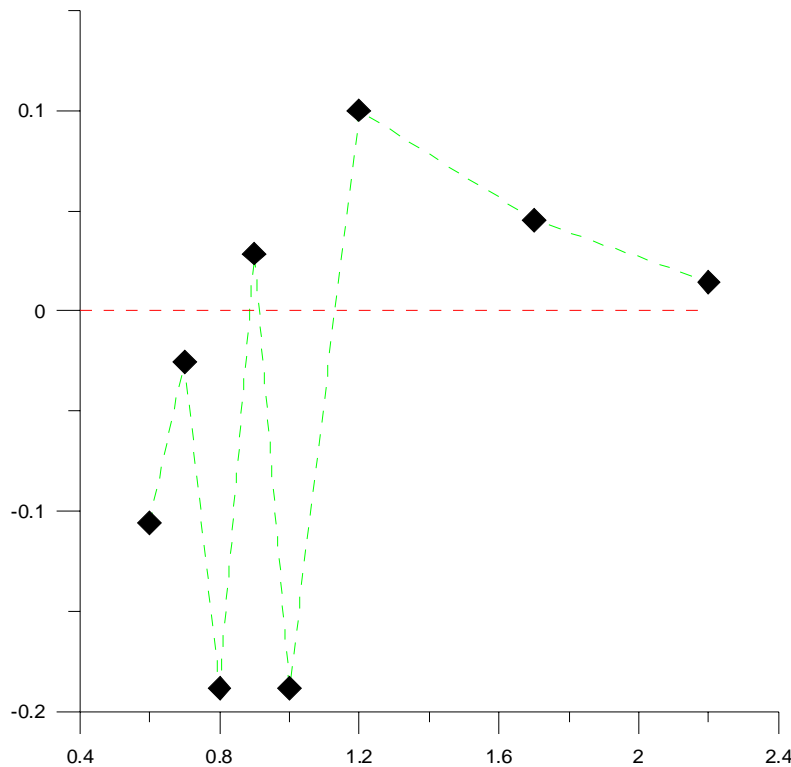

Figure 4. Influence of ground effect in the simulations, for A = 0, ω = 0, Re=10^5.

To better understand what is happening let us start analyzing the flow behind a stand still cylinder. From each side of the symmetry line (x-axis passing through the cylinder center) large structures formed by clusters of point vortices are shed alternately forming the Karmann vortex street. For low frequency of the body oscillation in ground effect (Case IV in Tab. 2), the behavior is almost the same although the positions of the cluster shedding move according to the oscillation amplitude; this is shown in Fig. 5.

Table 2: Results of C_L and C_D with ω=1.0 and Re = 10^5.

Case	A	ω	$\overline{C_L}$	$\overline{C_D}$	h/b	G_{min}
I	0	0	-0.07194976	1.28201151	0.7	0.2
II	0.05	1.0	-0.02525930	1.28331304	0.7	0.15
III	0.10	1.0	0.01069086	1.20050287	0.7	0.10
IV	0.15	1.0	0.12925778	1.09118962	0.7	0.05
V	0.05	1.0	-0.10624658	1.43586683	0.6	0.05
VI	0.05	1.0	-0.0252593	1.28331304	0.7	0.15
VII	0.05	1.0	-0.18872733	1.57669175	0.8	0.10
VII	0.05	1.0	0.02866777	1.23376429	0.9	0.25
IX	0.05	1.0	-0.18839182	1.45015180	1.0	0.45
X	0.05	1.0	0.10019104	1.26521969	1.2	0.65
XI	0.05	1.0	0.04547872	1.26271951	1.7	1.15
XII	0.05	1.0	0.01448197	1.15907335	2.2	1.65

For a heaving cylinder in the transition regime, the wake structure becomes intermittent and the vortex clusters are shed irregularly from the cylinder in ground effect.

Figure 6 is assembled with the data from the same simulation used in the Fig. 5; it is presented to illustrate the variation of lift and drag coefficients during the numerical simulation referred as Case IV in Tab. 2. As can be observed the lift coefficient oscillates with the same frequency of the circular cylinder. In this figure the green line is the cylinder motion and the red one is the lift coefficient. This phenomenon is the lock-in regime. This shows that the numerical method is able to predict the generation of lift force on an oscillating cylinder in lock-in regime.

Our simulation for the oscillating cylinder case, which moves with constant velocity in the presence of a ground plane, provided a very good estimate of lock-in regime. The amplitude of the oscillatory motion is considered to be small compared to the body length; therefore, to the first approximation one is allowed to transfer the body boundary condition from the actual position to a mean position of the body surface.
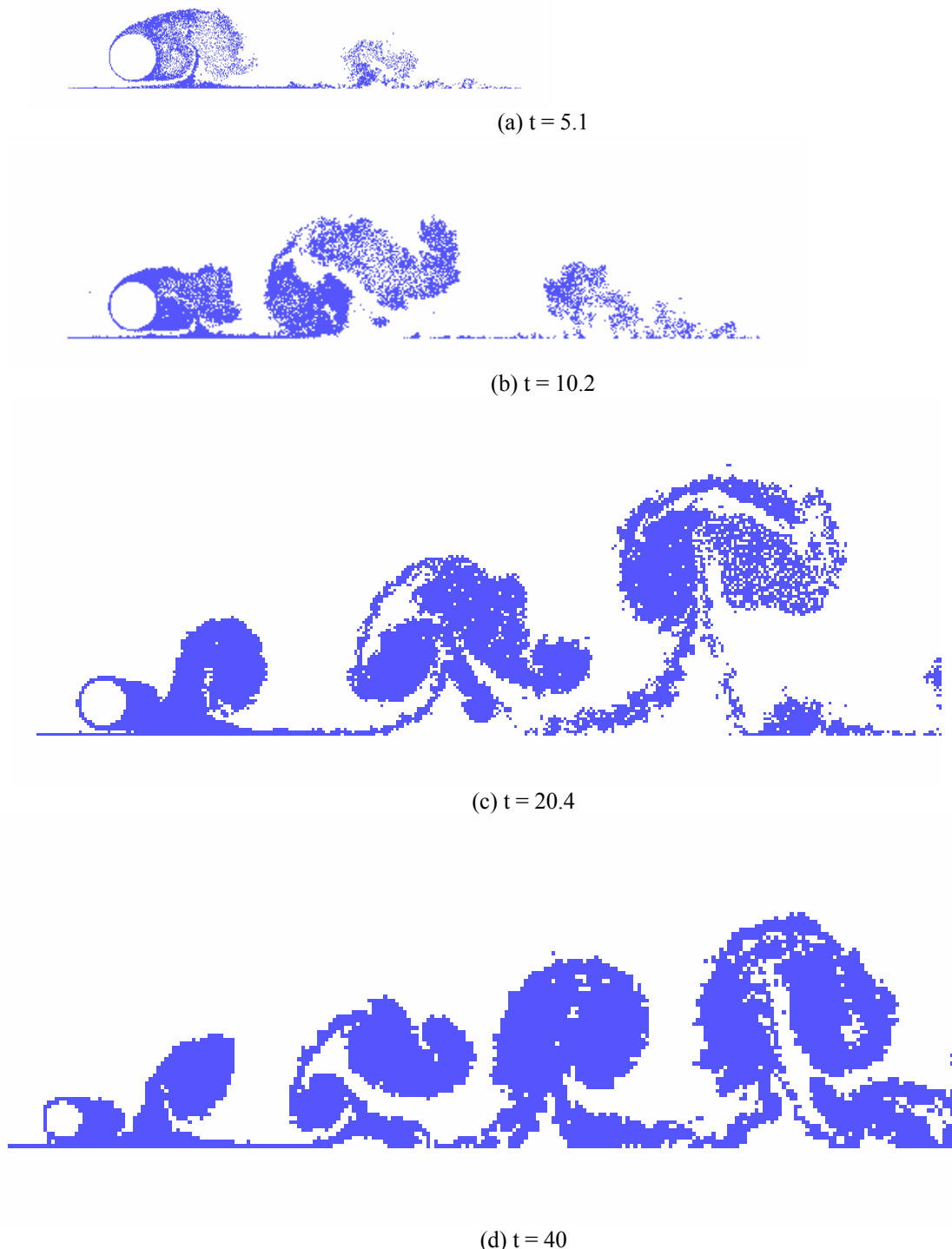

(a) t = 5.1

(b) t = 10.2

(c) t = 20.4

(d) t = 40

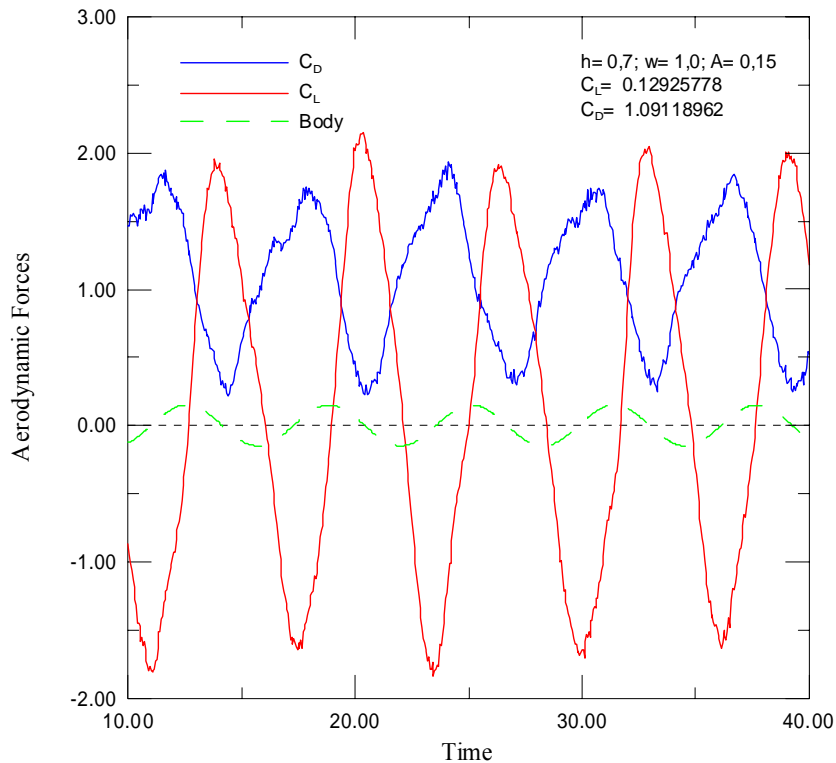Figura 5. Wake evolution for t= 5.1, t= 10.2, t= 20.4, t= 40 with A= 0.15, ω=1.0, h/b = 0.7 and Re = 10^5.

Figure 6: Lift coefficient during the numerical simulation with A= 0.15, ω=1.0, h/b = 0.7 and Re = 10^5.

As the results for a non-oscillating circular cylinder show the method developed here is very encouraging. It is capable of predicting very well the main global quantities inherent to the flow. The analysis of the influence of the numerical parameters on the simulation has pointed out the importance of choosing suitable values for M, A, ω and h/b. The influence of the numerical parameters on the simulation is extremely important and will be carried out.

The differences encountered in the comparison of the computed values with the experimental results for the distribution of the mean pressure coefficient along the cylinder surface as shown in Figure 3 are attributed mainly to the inherent three-dimensionality of the real flow for such a value of the Reynolds number, which is not modeled in the simulation. This seems to indicate that a higher value of M would improve the resolution and probably produce a better simulation with respect to the pressure distribution. More investigations are needed and one can imagine that with the use of more panels (and therefore more free vortices in the cloud) the results tend to be in closer agreement with the experiments.

The sub-grid turbulence modeling is of significant importance for the numerical simulation. The results of this analysis, taking into account the sub-grid turbulence modeling, are being generated and will be presented in due time, elsewhere.

Our simulation for the oscillating circular cylinder case provided a very estimative of the lock-in regime, and it needs further investigation.

5. Acknowledgement

6. References

Alcântara Pereira, L.A., Hirata, M.H. and Manzanares Filho, N. 2004, "Wake and Aerodynamics Loads in Multiple Bodies - Application to Turbomachinery Blade Rows", J. Wind Eng. Ind Aerodyn., 92, pp. 477-491.

Alcântara Pereira, L.A., Ricci, J.E.R., Hirata, M.H. and Silveira-Neto, A., 2002, "Simulation of Vortex-Shedding Flow about a Circular Cylinder with Turbulence Modeling", Intern'l Society of CFD, Vol. 11, No. 3, October, pp. 315-322.

Blevins, R.D., 1984, "Applied fluid dynamics hanbook", Van Nostrand Reinhold Co.

Chacaltana, J.T.A., Bodstein, G.C. R. and Hirata, M.H., 1995, "Analytical Sutdy of the Time-Dependent 2D Inteaction of a Thin Airfoil and a Vortex in the Presence of a Ground Plane", XIII Brazilian Congress of Mechanical Engineering - XIII COBEM - Belo Horizonte, MG, Brazil.

Chen, J.M. and Chang, D.M., 1997, "Unsteady Pressure Measuriments for Parallel Vortex-Airfoil Interaction at Low Speed", Journal of Aircraft, Vol. 34, No. 3, pp. 330-336.

Chorin, A.J., 1973, "Numerical Study of Slightly Viscous Flow", Journal of Fluid Mechanics, Vol. 57, pp. 785-796.

Ferziger, J.H., 1981, "Numerical Methods for Engineering Application", John Wiley & Sons, Inc.

Fonseca, G.F., Bodstein, G.C.R. and Hirata, M.H., 2003, "Numerical Simulation of Inviscid Incompressible Two-Dimensional Airfoil-Vortex Interaction in Ground Effect", Journal of Aircraft, Vol. 40, No. 4, July-August, pp. 653-661.

Fonseca, G.F., Bodstein, G.C.R. and Hirata, M.H., 1997, "A Numerical Inviscid Vortex Model Applied to Parallel Blade-Vortex Interaction", Journal of the Brazilian Society of Mechanical Sciences, Vol. 19, No. 3, pp. 341-356.

Kamemoto, K., 2004, "On Contribution of Advanced Vortex Element Methods Toward Virtual Reality of Unsteady Vortical Flows in the New Generation of CFD", Proceedings of the 10th Brazilian Congress of Thermal Sciences and Engineering-ENCIT 2004, Rio de Janeiro, Brazil, Nov. 29-Dec. 03, Invited Lecture-CIT04-IL04.

Kamemoto, K., 1993, "Procedure to Estimate Unstead Pressure Distribution for Vortex Method" (In Japanese), Trans. Jpn. Soc. Mech. Eng., Vol. 59, No. 568 B, pp. 3708-3713.

Lee, D.J. and Smith, C.A., 1991, "Effect of Vortex Core Distortion on Blade-Vortex Interaction", A.I.A.A. Journal, Vol. 29, No. 9, pp. 1355-1362.

Lewis, R.I., 1999, "Vortex Element Methods, The Most Natural Approach to Flow Simulation - A Review of Methodology with Applications", Proceedings of 1st Int. Conference on Vortex Methods, Kobe, Nov. 4-5, pp. 1-15.

Lewis, R. I., 1991, "Vortex Element Method for Fluid Dynamic Analysis of Engineering Systems", Cambridge Univ. Press, Cambridge, England, U.K..

McCune, J.E. and Tavares, T.S., 1993, "Perspective: Unsteady Wing Theory - The Karman/Sears Legacy", Journal of Fluids Engineering, Vol. 115, Dec., pp. 548-560.

Milne-Thompson, L.M., 1955, Theorical Hydrodynamics; MacMillan & Co.

Mook, D.T. and Dong, B., 1994, "Perspective: Numerical Simulations of Wakes and Blade-Vortex Interaction", Journal of Fluids Engineering, Vol. 116, March, pp. 5-21.

Mustto, A.A., Hirata, M.H. and Bodstein, G.C.R., 1998, "Discrete Vortex Method Simulation of the Flow Around a Circular Cylinder with and without Rotation", A.I.A.A. Paper 98-2409, Proceedings of the 16th A.I.A.A. Applied Aerodynamics Conference, Albuquerque, NM, USA, June.

Panaras, A.G., 1987, "Numerical Modeling of the Vortex/Airfoil Interaction", A.I.A.A. Journal, Vol. 25, No. 1, pp. 5-11.

Poling, D.R., Dadone, L. and Telionis, D.P., 1989, "Blade-Vortex Interaction", A.I.A.A. Journal, Vol. 27, No. 6, pp. 694-699.

Rai, M.M., 1987, "Navier-Stokes Simulations of Blade-Vortex Interaction Using High-Order Accurate Upwind Schemes", A.I.A.A. Paper 87-0543, November.

Ricci, J.E.R., Alcântara Pereira, L.A., Hirata, M.H. and Manzanares Filho, N., 2001, "Influence of a Ground Plane in the Aerodynamic Loads on an Airfoil" (In Portuguese), Proceedings of COBEM 2001, Fluid Mechanics, Vol. 8, pp. 130-138. Uberlândia, MG.

Sarpkaya, T., 1994, "Vortex Element Method for Flow simulation", Advances in applied Mechanics, Vol 31, pp. 113-247.

Seath, D.D., Kim, J.M. and Wilson, D.R., 1989, "Investigation of Parallel Blade-Vortex Interaction at Low Speed", Journal of Aircraft, Vol. 26, No. 4, pp. 328-333.

Shintani, M. and Akamatsu, T, 1994, "Investigation of Two Dimensional Discrete Vortex Method with Viscous Diffusion Model", Computational Fluid Dynamics Journal, Vol. 3, No. 2, pp. 237-254.

Silva, H., 2004, "Análise do Escoamento ao Redor de um Corpo Oscilante que se Desloca com Velocidade Constante". In Portuguese, UNIFEI, Itajubá, MG, Brasil, M.Sc. Dissertation.

Silva de Oliveira, L., Alcântara Pereira, L.A. and Hirata, M.H., 2005, "Numerical Simulation of the Airfoil – Vortex Cloud Interaction in Ground Effect", 18th International Congress of Mechanical Engineering, Proceedings of COBEM 2005, November 6-11, Ouro Preto, MG.

Silva de Oliveira, L., Alcântara Pereira, L.A., Hirata, M.H. and Manzanares Filho, N., 2004, "Numerical Modelling of the Airfoil-Vortex Cloud Interaction", Proceedings of the 10th Brazilian Congress of Thermal Sciences and Engineering - ENCIT 2004, Rio de Janeiro, Brazil, Nov. 29 - Dec. 03, Paper CIT04-0253.

Son, J.S., Hanratty, 1969, "Velocity Gradients at the Wall for Flow Around a Cylinder at Reynolds Number from $5x10^3$ to 10^5"; Journal of Fluid Mechanics, Vol. 35, no. 2, pp. 353-368.

Srinivasan, G.R. and McCroskey, W.J., 1993, "Euler Calculations of Unsteady Interaction of Advancing Rotor with a Line Vortex", A.I.A.A. Journal, Vol. 31, No. 9, pp. 1659-1666.

Straus, J., Renzoni, P. and Mayle, R.E., 1990, "Airfoil Pressure Measurement During a Blade Vortex Interaction and a Comparison with Theory", A.I.A.A. Journal, Vol. 28, No. 2, pp. 222-228.

Uhlman, J.S., 1992, "An Integral Equation Formulation of the Equation of an Incompressible Fluid", Naval Undersea Warfare Center, T.R. 10-086.